

# Prime and Modulate Learning: Generation of forward models with signed back-propagation and environmental cues

**Sama Daryanavard<sup>1</sup>, Bernd Porr<sup>1</sup>**

<sup>1</sup>Biomedical Engineering Division, School of Engineering, University of Glasgow, Glasgow G12 8QQ, UK.

## Abstract

Deep neural networks employing error back-propagation for learning can suffer from exploding and vanishing gradient problems. Numerous solutions have been proposed such as normalisation techniques or limiting activation functions to linear rectifying units. In this work we follow a different approach which is particularly applicable to closed-loop learning of forward models where back-propagation makes exclusive use of the *sign* of the error signal to prime the learning, whilst a global relevance signal modulates the rate of learning. This is inspired by the interaction between local plasticity and a global neuromodulation. For example, whilst driving on an empty road, one can allow for slow step-wise optimisation of actions, whereas, at a busy junction, an error must be corrected at once. Hence, the error is the priming signal and the intensity of the experience is a modulating factor in the weight change. The advantages of this Prime and Modulate paradigm is twofold: it is free from normalisation and it makes use of relevant cues from the environment to enrich the learning. We present a mathematical derivation of the learning rule in z-space and demonstrate the real-time performance with a robotic platform. The results show a significant improvement in the speed of convergence compared to that of the conventional back-propagation.

## 1 Introduction

Since its inception, deep learning has proven remarkably successful in a wide variety of areas, such as: image classification, speech recognition, and reinforcement learning Bahri et al. (2020). Deep Neural Networks (DNNs) employ activation functions, such as the logistic or the hyperbolic tangent ( $\tanh$ ), and are most commonly trained using an error signal with the Gradient Descent Method (GDM) for optimisation. The derivative of such functions have a narrow range of practical values and a limit of zero outwith,

therefore the propagation of the error signal through this non-linearity often suffers from the exploding and vanishing gradient problem (EVGP). This has ignited a significant research effort into addressing this issue; amongst the solutions are the network architectures such as long short-term memory (LSTM), precise weight initialisations, and specific non-linear activation functions (Hanin, 2018). Notably, linear rectifying units are used to remedy this problem which effectively remove the derivative and thus, drastically alter the behaviour of the network and the nature of learning. On the other hand, the logistic function allows for a smooth saturation of signals, along with  $\tanh$ . This is in accordance with neuroscience where nearly all psychometric functions or internal neuronal processing follow a sigmoid activation pattern.

From a neurophysiological standpoint, learning is driven by local and global mechanisms changing synaptic plasticity Reynolds and Wickens (2002). In particular, in closed-loop learning an interplay of local learning and global learning which has been advantageous, for example, improving the stability of learning when generating a forward model of a reflex Porr and Wörgötter (2007). Nonetheless, to date, this class of closed-loop learning has only been used in shallow networks, often with a single learning units or shallow networks (Porr and Wörgötter, 2007; Kulvicius et al., 2007; Maffei et al., 2017).

In this work, we present a learning paradigm that combines local error back-propagation and global modulation to create a robust learning scheme for the generation of forward models. More specifically, only the sign of the propagating signal is used to prime the nature of weight change in the context of their local connections, whilst a global “relevance” signal acts as a third factor to excite the weight changes across the network. This offers not only a robust, nearly one-shot real-time learning, free of exploding and vanishing gradient problem (EVGP), but also a more comparable learning model to neuroscience than the conventional back-propagation. In this paper, we implement this novel algorithm on a physical robot that learns to improve the performance of a closed-loop feedback controller (a *reflex*) by calculating its forward model, and thus prevents the triggering of the controller.

## 2 The closed-loop learning platform

**The reflex and predictive loops:** Figure 1 shows the learning platform. The so called “reflex” is a reactive closed loop controller which aims to stay as close to its desired state  $I_d$  as possible. This fixed reflex controller acts against the disturbance  $D$  which travels through the environmental transfer function  $R_E$ . This leads to a new state  $S$  that is picked up by  $R_S$  and causes a sensor signal  $I$ . This signal is compared to the desired state  $I_d$  at node ① and in turn creates the error signal  $E$ . This error signal is translated into an appropriate action  $A$  via the motor transfer function  $R_M$  to counteract the disturbance  $D$  at node ②. Here, the crucial aspect of the error signal  $E$  is that it can be used for *realtime* learning that enables the learner to generate a forward model of the reflex loop.

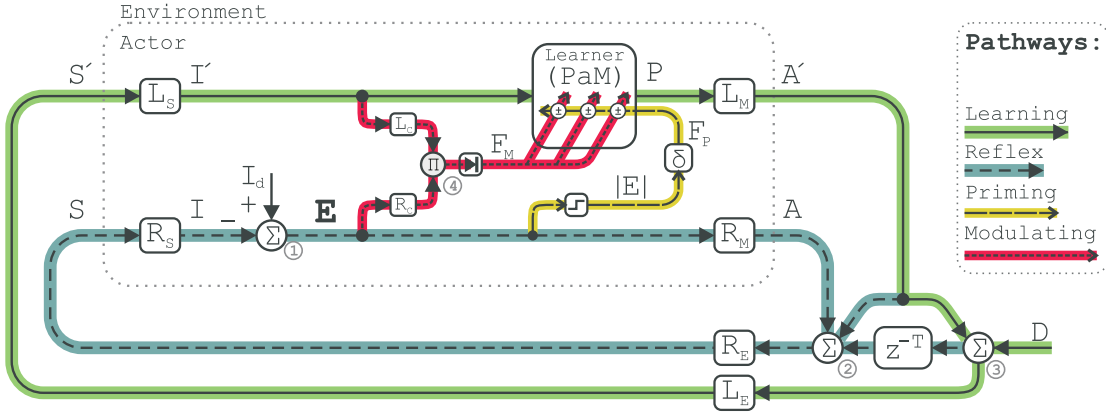


Figure 1: *The Prime and Modulate (PaM) closed-loop learning platform consisting of an inner reflex loop (highlighted in blue) and an outer learning loop (highlighted in green). The signal and transfer function notations are as follow: Disturbance ( $D$ ), delay function ( $z^{-T}$ ), reflex environment ( $R_E$ ), state of reflex ( $S$ ), reflex sensory unit ( $R_S$ ), reflex sensory input ( $I$ ), desired sensory input ( $I_d$ ), error signal ( $E$ ), reflex motor unit ( $R_M$ ), reflex motor action ( $A$ ), learner environment ( $L_E$ ), state of learner ( $S'$ ), learner sensory unit ( $L_S$ ), learner sensory input ( $I'$ ), learner ( $\text{PaM}$  network), learner motor action ( $A'$ ). The priming pathway is highlighted with red where  $F_P$  is the priming factor that propagates through the network. Modulating pathway is highlighted with yellow, where, reflex cue function ( $R_C$ ) and learner cue function ( $L_C$ ) lead to the modulating factor ( $F_M$ ) and drives the learning.*

Learning of the forward model is performed by the novel PaM network placed in the learning (predictive) loop. The disturbance travels through the learner's environment  $L_E$ , leading to a new state  $S'$  which is picked up by learner's sensory unit  $L_S$  and causes a predictive sensory signal  $I'$ . This is fed into the learning algorithm which in turn generates the output  $P$ . This is translated into the predictive action  $A'$ , executed by the learner's motor unit  $L_M$ , to eliminate the Disturbance  $D$  at node ③, before it can enter the reflex loop.

**z-space:** The signals in Figure 1 are discrete time and real-valued physical measurements, therefore are more accurately referred to as sequences. Due to the recursive nature of closed-loop systems it is beneficial to analyse their behaviour in z-space where discrete time-domain sequences are transformed into complex frequency-domain representations (Oppenheim, 1999). We use the unilateral z-transform representation of these sequences in this work, which, for an arbitrary sequence  $x[n]$ , is defined as:

$$X(z) = \mathcal{Z}\{x[n]\} = \sum_{n=0}^{\infty} (x[n]z^{-n}) \quad (1)$$

Where  $\mathcal{Z}\{\cdot\}$  is z-transform operator and  $z$  is a complex variable.

In this work we harness three properties of the z-transform: linearity, time shifting, and convolution of sequences (Oppenheim, 1999). This converts the recursive nature of the derivations into simple algebraic operations, for example considering the reflex loop and assuming that  $D$  and  $A'$  are zero, solving for the error signal yields:

$$\text{time-domain } \mathbf{e}[\mathbf{n}] = i_d(t) - r_S(r_E(r_M(e[n-1]))) \quad (2)$$

$$\text{z-space } \mathbf{E}(z) = I_d(z) - R_S R_E R_M \cdot z^{-1} E(z) = \frac{I_d}{1 + R_S R_E R_M z^{-1}} \quad (3)$$

This shows that the error signal is function in time-domain, whereas, with z-transformation this translates into multiplication of transfer functions and sequences which allows for expression of  $E(z)$  to be derived. In this work the  $(z)$  symbol, representing the complex variable, is omitted for brevity.

**The prime and modulate pathways:** As described in the introduction, only the sign of the error signal  $E$  is used to generate the priming factor ( $F_P$ ) for the back-propagation (BP), while the global modulating factor ( $F_M$ ) acts as a third factor where a filtered version of the sensor inputs is used as a novelty or relevance signal which modulates the learning with its amplitude. This is in line with the claim that in particular dorsal striatal dopamine is more of a novelty or salience detector Prescott et al. (2006) than an error signal, or serotonin being a rectified version of the reward prediction error Li et al. (2016). These signals and their functionalities are described in more details in the future sections.

**The learning goal:** The aim of the learner is to produce a predictive signal  $P$  such that the error signal  $E$  is kept at zero persistently. In mathematical terms, this is analogous to minimising the absolute value of the error  $|E|$ ; since this is a non differentiable function at  $E = 0$  the quadratic of  $E$  is minimised instead:

$$\text{Learning goal: } P = \underset{p}{\text{arg min}} E^2 \quad (4)$$

This is achieved by adjusting the internal parameters of the network that are introduced below.

**The neural network:** This paradigm employs a feed-forward neural network with fully connected layers. Figure 2 shows the internal connections of two neurons in this network.

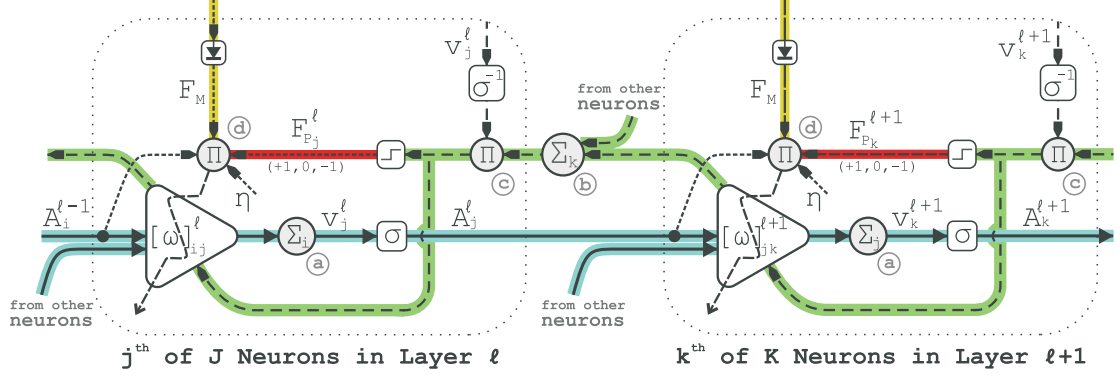


Figure 2: Neuron connections in PaM network. Forward propagation of inputs is shown with the left-to-right solid lines highlighted in blue.  $\sigma$  is the sigmoid activation function and  $A_j^\ell$  denotes the activation of  $j^{\text{th}}$  neuron in layer  $\ell$ .  $[\omega]_{ij}^\ell$  is the weight matrix associated with inputs  $I$  inputs to this layer. The summation node (a) corresponds to Equation 5. Backpropagation pathway is shown with right-to-left dashed lines highlighted in green. The summation at node (b) and product at node (c) correspond to Equation 10. The priming pathway is shown with short dashed lines highlighted in red. This is the sign of the resulting value from the backpropagation pathway, see Equation 11. The modulating pathway is shown in long dashed lines that enter each neuron from the environment, see Equation 12. The priming and modulating factors join at node (d), together with the learning rate  $\eta$  and the relevant input to the neuron  $A_i^{\ell-1}$ , to drive the learning rule, corresponding to Equation 13.

The forward propagation of activations  $A$  is shown with solid right-arrows and is calculated as:<sup>1</sup>

$$A_j^\ell = \sigma(v_j^\ell) = \sigma(\sum_{i=1}^I \omega_{ij}^\ell \sigma(v_i^{\ell-1})) = \sigma(\sum_{i=1}^I \omega_{ij}^\ell A_i^{\ell-1}) \text{ Where: } \ell = 1 \rightarrow L \quad (5)$$

Where  $\omega$  denotes the weights,  $v$  is referred to as the sum output, and the  $\sigma$  is the logistic function that maps the sum output of the neuron  $v$  to the activation. The weighted sum takes place at summation points (a). Note that for  $\ell = 1$ , the predictive input information substitute for the input activations:  $A_i^0 = I_i^0$  and, for  $\ell = L$ , the weighted sum of activations in the last layer yields the predictive signal in the closed-loop platform:  $P = \sum_{x=0}^X (g_x A_x^L)$ , where  $g_x$  is a weighting constant.

### 3 Derivation of the learning rule

The learning goal in Equation 4 is achieved through adjustments of weights  $\omega$  in Equation 5. At each iteration, the error signal  $E$  provides the network with constructive feedback on the adequacy of the predictive signal  $P$ . Conventionally, the GDM is employed for weight optimisation; where the change to an arbitrary weight is proportional

<sup>1</sup>The superscripts denote the layer index, the first subscripts denote the neuron index, and the second subscripts denote the input (or the associated weight) index.

to the sensitivity of  $E^2$  with respect to the sum output  $v$  of the neuron containing that weight:

$$\text{Gradient descent method: } \Delta\omega_{ij}^\ell \propto \frac{\partial E^2}{\partial v_j^\ell} \quad (6)$$

When differentiating in z-space we assume that the weight changes in time-domain are constant or significantly slower than the changes in the closed-loop system. (reference??). We seek an expression of this gradient in the context of closed-loop applications. With a similar approach to Daryanavard and Porr (2020), this gradient is unravelled using the chain rule:

$$\frac{\partial E^2}{\partial v_j^\ell} = \overbrace{\frac{\partial E^2}{\partial P}}^{\text{Closed-loop}} \cdot \overbrace{\frac{\partial P}{\partial v_j^\ell}}^{\text{Network}} \quad (7)$$

The former partial derivative solely relates to the dynamics of the closed-loop platform, whilst, the latter partial derivative relates to the inner connections of the network.

**The closed-loop gradient ( $\frac{\partial E^2}{\partial P}$ ):** Referring to Figure 1 (summation points ① and ②), the closed-loop expression of the error signal in z-space is derived as:

$$\begin{aligned} \mathbf{E} &= I_d - I = I_d - R_S R_E \left( \overbrace{\mathbf{E} R_M}^{=A} + \overbrace{P L_M}^{=A'} + D z^{-T} \right) \\ &= \frac{I_d - R_S R_E (P L_M + D z^{-T})}{1 + R_S R_E R_M} \end{aligned} \quad (8)$$

Therefore, differentiation of quadratic of  $E$  with respect to  $P$  yields:

$$\text{Closed-loop gradient: } \frac{\partial E^2}{\partial P} = 2E \frac{\partial E}{\partial P} = 2E \frac{-R_S R_E L_M}{1 + R_S R_E R_M} \quad (9)$$

The value of the resulting fraction can be found experimentally by substituting  $I_d = 0$ ,  $D = 0$ , and  $P = 1$  in Equation 8 and measuring  $E$ ; this is the closed loop gain of the system.

**The network gradient ( $\frac{\partial P}{\partial v}$ ):** From Equation 5, differentiating with respect to an arbitrary sum output  $v_j^\ell$  results in a recursive expression:

$$\text{Network gradient: } \frac{\partial P}{\partial v_j^\ell} = \sigma^{-1}(v_j^\ell) \cdot \sum_{k=0}^K (\omega_{jk}^{\ell+1} \frac{\partial P}{\partial v_k^{\ell+1}}) \quad (10)$$

Where  $\sigma^{-1}$  is the inverse logistic function. For the neurons in the final layer we have:  $P = A_x^L$ , therefore, this gradient is simply calculated as:  $\sigma^{-1}(v_x^L)$ . This is fed through

the network using the back-propagation technique. This chain of events is shown by dashed left-arrows in Figure 2, with the weighted sum and the product indicated at points ⑥ and ⑦, respectively.

With that, we have an expression of the gradient found in Equation 6 which can be used for closed-loop learning applications. However, depending on the distribution of the weights and the topology of the neural network, the propagation can suffer from exploding and vanishing gradient problem (Pascanu et al., 2013; Bengio et al., 1994, 1993). In the following section we derive the PaM learning rule which is free from this issue.

**Prime and Modulate learning** In this work merely the *sign* of the gradient  $\frac{\partial E^2}{\partial v}$ , found in Equation 6, is used for learning. This serves to 'prime' the weights to later undergo an increase, a decrease, or remain unchanged. Hence, it is referred to as the Priming Factor  $F_P$  as seen in Figures 1 and 2:

$$F_P = \delta(E) = \frac{\frac{\partial |E|^2}{\partial v}}{\left| \frac{\partial |E|^2}{\partial v} \right|} = \begin{cases} +1 & \text{primes } \omega \text{ to be increased} \\ 0 & \text{primes } \omega \text{ to remain unchanged} \\ -1 & \text{primes } \omega \text{ to be decreased} \end{cases} \quad (11)$$

Once primed, the magnitude of weight change is dictated by a secondary signal that contains collective cues gathered from the environment informing the significance and/or relevance of the learning experience at any given instance of time.  $R_C$  and  $L_C$ , shown in Figure 1, are functions designed to extract relevant cues from the reflex and predictive loops, respectively. The correlation of these cues indicated at product point ④, modulates the magnitude of weight changes. Hence, this signal is referred to as the Modulating Factor  $F_M$  (Figures 1 and 2):

$$F_M = |ER_C \cdot I'L_C| \quad (12)$$

Finally, we redefine the weight change proportionality in Equation 6, and with the introduction of the learning rate  $\eta$ , we establish the update rule for this paradigm (refer to Equations 5, 7, and 9):

$$\Delta\omega_{ij}^\ell \propto \overbrace{\frac{2E \cdot \frac{-R_S R_E L_M}{1+R_S R_E R_M} \cdot \frac{\partial P}{\partial v_i^\ell}}{\left| 2E \cdot \frac{-R_S R_E L_M}{1+R_S R_E R_M} \cdot \frac{\partial P}{\partial v_i^\ell} \right|}}^{\text{priming factor}} \cdot \overbrace{|ER_C \cdot I'L_C|}^{\text{modulating factor}}$$

$$\Delta\omega_{ij}^\ell := \eta A_i^{\ell-1} F_{P_j}^\ell F_M \quad (13)$$

As explained above,  $F_{P_j}^\ell$  is back-propagated through the layers, whilst,  $F_M$  is available to all neurons in the network globally; Figure 2 point ④ illustrates the weight changes. This finalises the derivation of the learning rule for Prime and Modulate (PaM) paradigm.

## 4 Experimentation platform: robotic navigation

Figure 3 illustrates the experimental setup where a robot is placed on a canvas with the task of following a path. The robot is fitted with a Raspberry Pi 3B+ (RPi) that hosts the learning algorithm as an external C++ library. The network is initialised with 10 hidden layers for the following set of experiments.

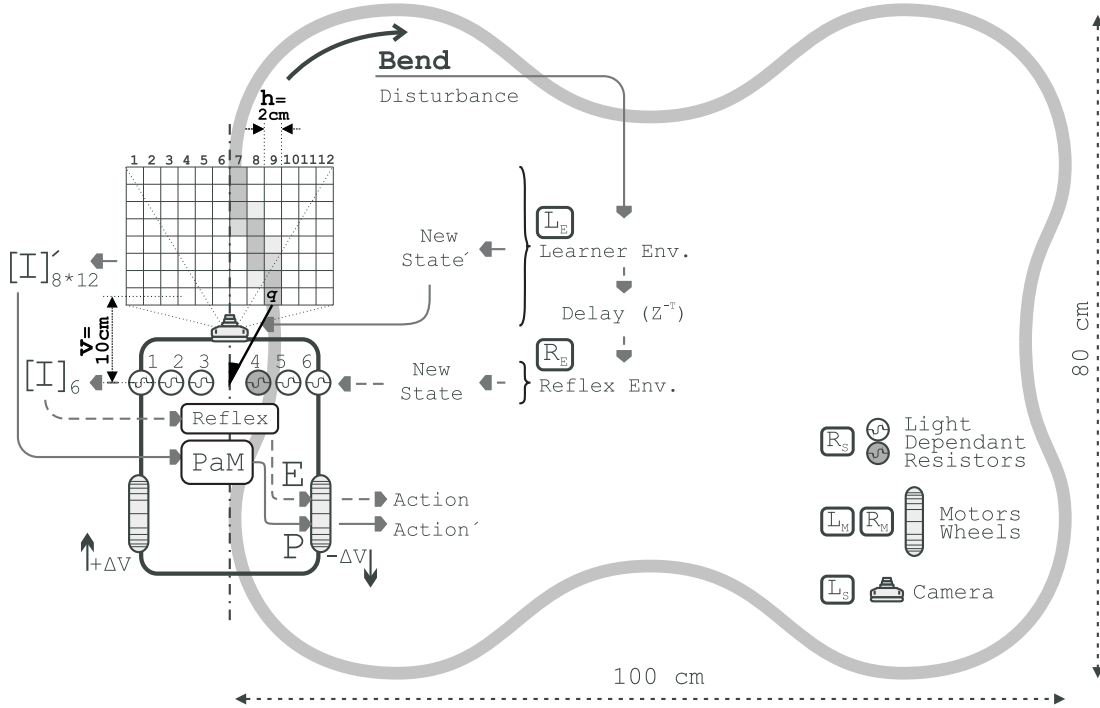


Figure 3: Schematic of the experimental setup: A robot placed on a canvas which navigates the path

The chassis houses an array of Light Dependent Resistors (LDRs), a camera, two wheels with servo motors, and a battery bank to power the system. The equivalent closed-loop symbol of these components, as introduced in Figure 1, are shown here.

**Light Dependent Resistors:** These sensors measure the Grey-Scale Values (GSVs)  $I_i$  of the surface underneath them and thus, monitor the position of the robot with respect to the path. The desired state is a symmetrical stand, therefore, a nonsymmetrical alignment results in the generation of a non-zero error signal as:

$$E = a(I_1 - I_6) + b(I_2 - I_5) + c(I_3 - I_4) \quad \text{where: } a > b > c \quad (14)$$

The weighting registers the degree of deviation and enables sharp, medium, or gentle steering.

**Servo motors:** This error signal is used to recover the desired symmetrical state by altering the speed of motors:



$$\begin{aligned}
V_{left} &= V_0 - \overbrace{dE}^{Reflex} - \overbrace{eP}^{Network} = V_0 - \Delta V \\
V_{right} &= V_0 + \Delta V
\end{aligned} \tag{15}$$

Where  $V_0 = 7[\frac{cm}{s}]$  and  $d$  is an experimental constant. This describes the functionality of the reflex loop in this application.

**The camera** The view of the road ahead is captured by the camera in the form of a matrix of GSVs  $[I]_{8*12}'$  and is fed into the neural network.

In addition to the error signal, the predictive output of the network  $P$  is used for steering as in Equation 15, where  $e$  is a scaling factor found experimentally. The error signal in Equation 14 is used to train the network. Below, we derive the learning rule for this application.

**The priming factor:** The closed loop gain derived in Equation 9 is found to be  $\approx 0.97$  for this setup. Therefore, the Priming Factor for this learning is:  $F_P = 1.94E\frac{\partial P}{\partial v}$ . Where the error signal and the partial derivative are calculated from Equations 14 and 10, respectively.

**The modulating factor:** When  $E > 0$ , a positive change indicates further deviation whilst a negative change implies recentering. In contrary, when  $E < 0$ , a negative change indicates further deviation from the path whilst a positive change implies recentering. Therefore, the product of the two,  $E\frac{\partial E}{\partial t}$ , signals the worsening or bettering of the performance when its value is positive or negative, respectively. The exponential of this product is the cue extracted from the reflex inputs  $[I]_6$  signifying the learning at each iteration:  $E \cdot R_C = e^{E\frac{\partial E}{\partial t}}$

Thus the learning is weakly modulated when the navigation is improving and is strongly modulated as the navigation worsens. The cue extracted from the predictive inputs  $[I]_{8*12}'$  is the angle of deviation. The vertical distance of the bottom row of this matrix to the sensors' location  $v$  and the horizontal spread  $h$  of each pixel are measured. By having the index  $q$  of the pixel that captures the path the angle of deviation is found as:  $I' \cdot L_C = \arctan \frac{h \cdot |6.5 - q|}{v}$

The modulating factor is defined as the correlation of the aforementioned cues. Therefore, the update rule for this application is:

$$\Delta\omega_{ij}^\ell := \eta A_i^{\ell-1} \cdot 1.94E \frac{\partial P}{\partial v_j^\ell} \cdot e^{E\frac{\partial E}{\partial t}} \cdot \arctan \frac{h \cdot |6.5 - q|}{v} \tag{16}$$

## 5 Results: comparison of GDM and PaM

The performance of PaM paradigm is compared to that of the closed-loop GDM benchmarked in Daryanavard and Porr (2020). Successful learning is defined as the state

where the error's moving average over 10 seconds,  $0.1 \int_{t-10}^t |E| dt$ , falls below 1% of its maximum value during the trial.

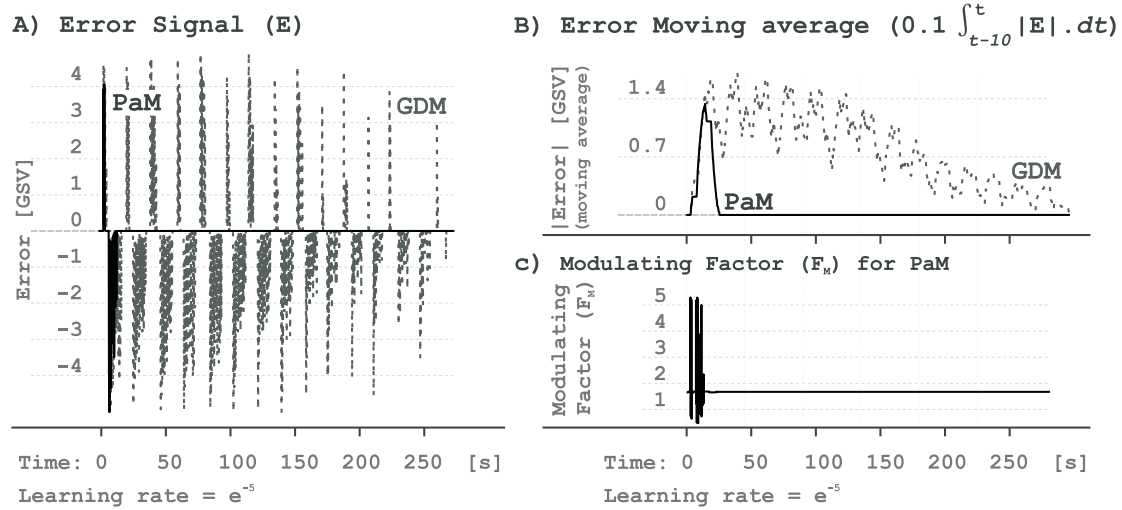


Figure 4: A pair of comparative learning trials with learning rate of  $\eta = e^{-5}$

The dashed traces in Figure 4A and B show the error signal  $E$  and its moving average during a GDM trial with the learning rate<sup>2</sup> of  $\eta = e^{-5}$ ; the success condition is reached at time  $t = 266.3[s]$ . The black traces in these figures show the error signal  $E$  and its moving average during a trial with PaM; the success condition is achieved at time  $t = 23.1[s]$ . The modulating factor  $F_M$  for this trial is shown in figure 4C. This pair of trials shows a significant improvement in the speed of learning and navigational performance of the robot.

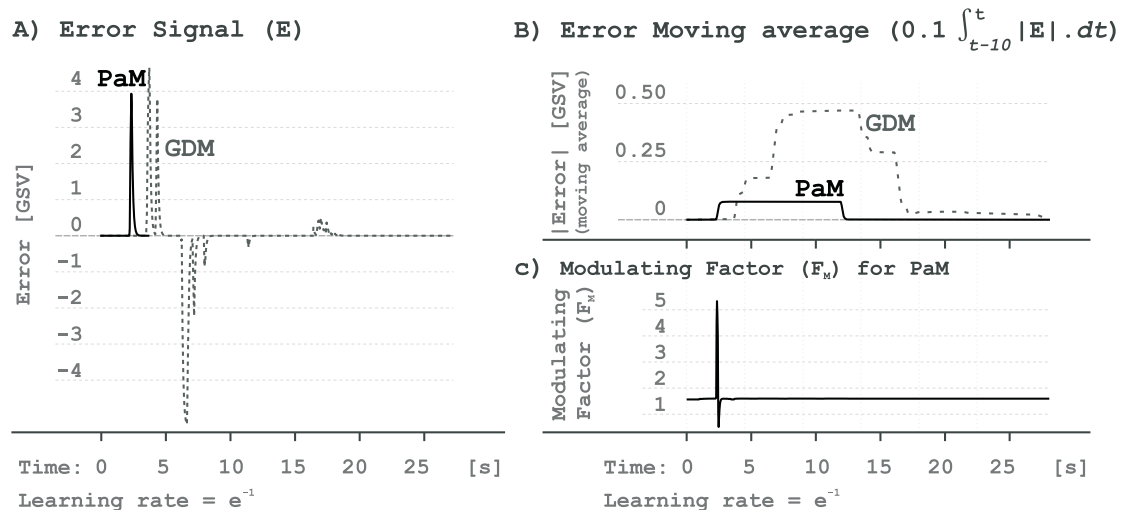


Figure 5: A pair of comparative learning trials with learning rate of  $\eta = e^{-1}$

A second pair of trials with higher learning rate of  $\eta = e^{-1}$  is shown in figure 5; this

<sup>2</sup>This is the natural number  $e = 2.71828$

shows a close to one-shot learning performance for PaM. Such comparative trial pairs were repeated 50 times across learning rates of:  $\eta = [e^{-5}, e^{-4}, e^{-3}, e^{-2}, e^{-1}]$ .

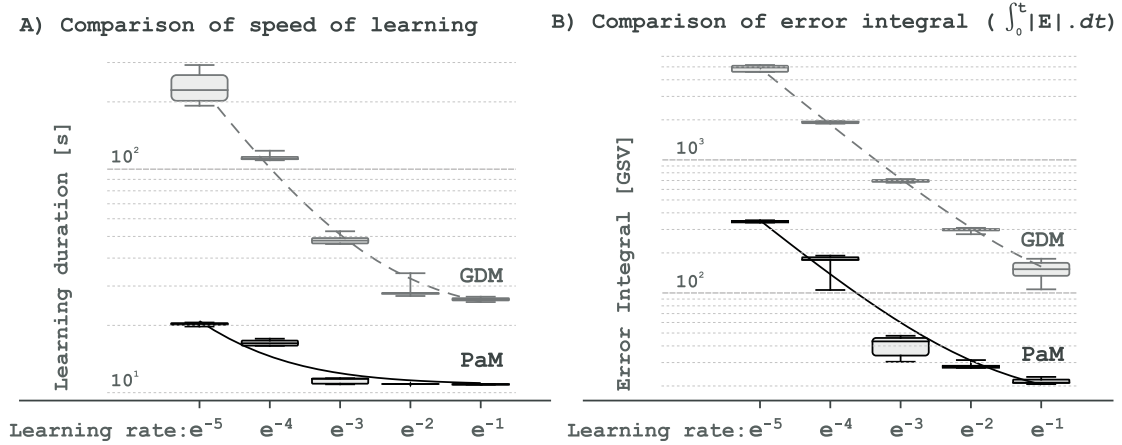


Figure 6: *comparison of learning speed and total error over a range of 5 different learning rates*

Figure 6A shows the time taken for the robot to obtain the success state during the trials with PaM (black trace) compared to that of the GDM (dashed trace). This shows consistency in the trend observed in Figures 4 and 5, in that, the PaM paradigm is significantly faster than its GDM counterpart. Both methods demonstrate a faster learning with higher learning rates, however, the performance of GDM is influenced by changes in the learning rate to a greater degree, given by the deflection of the fitted curve. Figure 6B show the corresponding error integrals,  $\int_0^t |E| dt$ , for these trials. As anticipated, the accumulation of the error signal is greater in trials with slower learning rate. Although the total accumulation of error is significantly smaller in PaM trials, in both methods this parameter is influenced by the learning rates to the same degree; inferred from the slope of the fitted curves.

## 6 Discussion

In this work we presented a novel closed loop algorithm which learns the forward model of a reflex Porr and Wörgötter (2003). These models play an important role in robotic and biological motor control (Wolpert and Kawato, 1998; Wolpert et al., 2001; Haruno et al., 2001; Nakanishi and Schaal, 2004) where they guarantee, for example, an optimal trajectory. Previous work in this area used shallow networks (Kulvicius et al., 2007), filter banks Porr and Wörgötter (2003) or single layers to perform predictive control (Nakanishi and Schaal, 2004; Maffei et al., 2017) and it was not possible to employ deeper structures. On the other hand, model free closed-loop learning has been using more complex network structures such as deep learning in combination with Q-learning (Guo et al., 2014; Bansal et al., 2016). Here, we demonstrate that model based closed-loop learning can also benefit from deep learning and thus a combination of both is more powerful (Botvinick et al., 2019). However, given the fast learning of this

model it can be prone to converging to a local minima. Whether or not deep learning is biologically realistic has been debated for many years where the main issue is the requirement of weight symmetry for forward- and backward-pass which limits its plausibility to only a few layers Lillicrap et al. (2016). However, if the error is merely transmitted as a sign, this weight symmetry can be relaxed as long as there are interconnections between the top/down and bottom/up pathways guaranteeing the correct sign of the learning Larkum (2013). In the context of neuroscience, this means that the bottom up pathway just controls long term potentiation (LTP) or long term depression (LTD) while neuromodulators, in particular serotonin as a rectified reward prediction error, can control the speed of the learning Iigaya et al. (2018) as a third factor (Li et al., 2016). Thus, in particular for cortical processing where serotonin is more prominent than dopamine and deep neuronal structures exist, a combination of local and global learning is a compelling fit for neuroscience, in addition to its application in machine learning and robotic navigation.

## Acknowledgements

We would like to acknowledge Jarez Patel for his valuable intellectual and technical input for the making of the robotic platform.

## References

- Bahri, Y., Kadmon, J., Pennington, J., Schoenholz, S. S., Sohl-Dickstein, J., and Ganguli, S. (2020). Statistical mechanics of deep learning. *Annual Review of Condensed Matter Physics*.
- Bansal, S., Akametalu, A. K., Jiang, F. J., Laine, F., and Tomlin, C. J. (2016). Learning quadrotor dynamics using neural network for flight control. In *2016 IEEE 55th Conference on Decision and Control (CDC)*, pages 4653–4660. IEEE.
- Bengio, Y., Frasconi, P., and Simard, P. (1993). The problem of learning long-term dependencies in recurrent networks. In *IEEE international conference on neural networks*, pages 1183–1188. IEEE.
- Bengio, Y., Simard, P., and Frasconi, P. (1994). Learning long-term dependencies with gradient descent is difficult. *IEEE transactions on neural networks*, 5(2):157–166.
- Botvinick, M., Ritter, S., Wang, J. X., Kurth-Nelson, Z., Blundell, C., and Hassabis, D. (2019). Reinforcement learning, fast and slow. *Trends in cognitive sciences*.
- Daryanavard, S. and Porr, B. (2020). Closed-loop deep learning: Generating forward models with backpropagation. *Neural Computation*, 32(11):2122–2144.
- Guo, X., Singh, S., Lee, H., Lewis, R. L., and Wang, X. (2014). Deep learning for real-time atari game play using offline monte-carlo tree search planning. In Ghahramani, Z., Welling, M., Cortes, C., Lawrence, N. D., and Weinberger, K. Q., editors,

- Advances in Neural Information Processing Systems 27*, pages 3338–3346. Curran Associates, Inc.
- Hanin, B. (2018). Which neural net architectures give rise to exploding and vanishing gradients? *arXiv preprint arXiv:1801.03744*.
- Haruno, M., Wolpert, D. M., and Kawato, M. (2001). Mosaic model for sensorimotor learning and control. *Neural computation*, 13(10):2201–2220.
- Iigaya, K., Fonseca, M. S., Murakami, M., Mainen, Z. F., and Dayan, P. (2018). An effect of serotonergic stimulation on learning rates for rewards apparent after long intertrial intervals. *Nature Communications*, 9(1):2477.
- Kulvicius, T., Porr, B., and Wörgötter, F. (2007). Chained learning architectures in a simple closed-loop behavioural context. *Biological Cybernetics*, 97(5-6):363–378.
- Larkum, M. (2013). A cellular mechanism for cortical associations: an organizing principle for the cerebral cortex. *Trends in neurosciences*, 36(3):141–151.
- Li, Y., Zhong, W., Wang, D., Feng, Q., Liu, Z., Zhou, J., Jia, C., Hu, F., Zeng, J., Guo, Q., Fu, L., and Luo, M. (2016). Serotonin neurons in the dorsal raphe nucleus encode reward signals. *Nature Communications*, 7(1):10503.
- Lillicrap, T. P., Cownden, D., Tweed, D. B., and Akerman, C. J. (2016). Random synaptic feedback weights support error backpropagation for deep learning. *Nature communications*, 7:13276.
- Maffei, G., Herreros, I., Sanchez-Fibla, M., Friston, K. J., and Verschure, P. F. (2017). The perceptual shaping of anticipatory actions. *Proceedings of the Royal Society B: Biological Sciences*, 284(1869):20171780.
- Nakanishi, J. and Schaal, S. (2004). Feedback error learning and nonlinear adaptive control. *Neural Networks*, 17(10):1453–1465.
- Oppenheim, A. V. (1999). *Discrete-time signal processing*. Pearson Education India.
- Pascanu, R., Mikolov, T., and Bengio, Y. (2013). On the difficulty of training recurrent neural networks. In *International conference on machine learning*, pages 1310–1318.
- Porr, B. and Wörgötter, F. (2003). Learning a forward model of a reflex. In Becker, S., Thrun, S., and Obermayer, K., editors, *Advances in Neural Information Processing Systems*, volume 15. MIT Press.
- Porr, B. and Wörgötter, F. (2007). Learning with “Relevance”: Using a Third Factor to Stabilize Hebbian Learning. *Neural Computation*, 19(10):2694–2719.
- Prescott, T. J., González, F. M. M., Gurney, K., Humpries, M. D., and Redgrave, P. (2006). A robot model of the basal ganglia: Behaviour and intrinsic processing. *Neural Networks*, In Press.

- Reynolds, J. N. and Wickens, J. R. (2002). Dopamine dependent plasticity of corticostriatal synapses. *Neural Networks*, 15:507–521.
- Riedmiller, M. and Braun, H. (1993). A direct adaptive method for faster backpropagation learning: The rprop algorithm. In *IEEE international conference on neural networks*, pages 586–591. IEEE.
- Wolpert, D. M., Ghahramani, Z., and Flanagan, J. R. (2001). Perspectives and problems in motor learning. *Trends in cognitive sciences*, 5(11):487–494.
- Wolpert, D. M. and Kawato, M. (1998). Multiple paired forward and inverse models for motor control. *Neural networks*, 11(7-8):1317–1329.